

# Articles

## Mesoporous Silica Spheres as Supports for Enzyme Immobilization and Encapsulation

Yajun Wang and Frank Caruso\*

Centre for Nanoscience and Nanotechnology, Department of Chemical and Biomolecular Engineering,  
The University of Melbourne, Victoria 3010, Australia

Received September 27, 2004. Revised Manuscript Received November 22, 2004

We report the immobilization of various enzymes in mesoporous silica (MS) spheres followed by encapsulation via the layer-by-layer assembly of multilayered nanocomposite thin shells. A range of enzymes with different molecular sizes and isoelectric points (pI) (e.g., catalase, peroxidase, cytochrome C, and lysozyme) has been examined in MS particles with a series of pore sizes. MS spheres with a bimodal mesoporous structure (BMS, 2–3 nm and 10–40 nm) show faster immobilization rates and significantly improved enzyme immobilization capacity than similar particles with only the smaller mesopores. High enzyme loadings (20–40 wt %) and rapid uptake (several minutes) were observed in BMS spheres for enzymes with a molecular size  $\leq 3$  nm and  $pI \geq 10$ . Following immobilization of the enzyme catalase, multilayered polyelectrolyte (PE) [poly(diallyldimethylammonium chloride), PDDA/poly(sodium 4-styrenesulfonate), PSS], or PE/nanoparticle [PDDA/silica nanoparticles,  $Si_{NP}$ ] shells were deposited onto the enzyme-loaded spheres. The activity of the encapsulated catalase was retained, even after exposure to enzyme-degrading substances (e.g., proteases). Catalase also exhibits enhanced stability in reaction conditions over a wide pH range (pH 5–10) and retains an activity of 70% after 25 successive batch reactions, demonstrating the usefulness of the loaded particles in biocatalytic applications. The PDDA/PSS multilayer-encapsulated catalase in BMS spheres shows a lower activity than catalase encapsulated by PDDA/ $Si_{NP}$  multilayers. However, the enzyme possesses significantly enhanced reaction stability with increasing PDDA/PSS layer number, which might be caused by a reduced reaction rate. The approach presented provides a general strategy for the encapsulation of macromolecules in MS materials.

### Introduction

The widespread interest in enzyme immobilization has largely been driven by the benefits of immobilized enzymes with respect to enhanced stability, repeated use, facile separation from reaction mixtures, and the prevention of enzyme contamination in products.<sup>1</sup> The commonly used immobilization methods may be subdivided into three general classes according to the forces involved: chemical bonds, where covalent bonds are formed with the enzyme;<sup>2</sup> physical adsorption, where hydrogen bonding, and electrostatic and hydrophobic interactions between support and enzyme exist;<sup>3</sup> and physical entrapment, for example, by sol–gel or polyelectrolyte (PE) multilayer entrapment.<sup>4</sup> Both inorganic and organic materials, such as porous glass, cellulose, chitosan, silica gels, polystyrene colloidal particles, and hydrogels, are often used as supports for enzyme immobilization.

Mesoporous silicas (MSs) are porous materials with extremely high surface areas and pore sizes in the range of 2–50 nm.<sup>5</sup> The pore sizes of MS are comparable to the diameter of enzymes, and for this reason these materials have begun to attract attention as supports for enzyme immobilization.<sup>6–9</sup> Two general problems have often been reported in the use of MS as supports for enzyme immobilization. The first is related to MCM-41 materials (pore sizes ca. 2–8

\* Corresponding author: Fax: +61 3 8344 4153. E-mail: fcaruso@unimelb.edu.au.

(1) Bornscheuer, U. T. *Angew. Chem., Int. Ed.* **2003**, *42*, 3336.

(2) Cetinus, S. A.; Oztop, H. N. *Enzyme Microb. Technol.* **2003**, *32*, 889.

(3) (a) Avnir, D.; Braun, S.; Lev, O.; Ottolenghi, M. *Chem. Mater.* **1994**, *6*, 1605. (b) Livage, J.; Coradin, T.; Roux, C. *J. Phys.: Condens. Matter* **2001**, *13*, 673.

(4) (a) *Protein Architecture: Interfacing Molecular Assemblies and Immobilization Biotechnology*; Lvov, Y., Möhwald, H., Eds.; Marcel Dekker: New York, 2000. (b) Wei, Y.; Xu, J.; Feng, Q.; Dong, H.; Lin, M. *Mater. Lett.* **2000**, *44*, 6. (c) Gill, I.; Ballesteros, A. *J. Am. Chem. Soc.* **1998**, *120*, 8587. (d) Caruso, F.; Niikura, K.; Furlong, D. N.; Okahata, Y. *Langmuir* **1997**, *13*, 3427.

(5) (a) Yanagisawa, T.; Shimizu, T.; Kuroda, K.; Kato, C. *Bull. Chem. Soc. Jpn.* **1990**, *63*, 988. (b) Kresge, T.; Leonowicz, M. E.; Roth, W. J.; Vartuli, J. C.; Beck, J. S. *Nature* **1992**, *359*, 710.

(6) (a) Yiu, H. H. P.; Wright, P. A.; Botting, N. P. *Microporous Mesoporous Mater.* **2001**, *44–45*, 763. (b) Yiu, H. H. P.; Wright, P. A.; Botting, N. P. *J. Mol. Catal. B: Enzymol.* **2001**, *15*, 81. (c) Takahashi, H.; Li, B.; Sasaki, T.; Miyazaki, C.; Kajino, T.; Inagaki, S. *Chem. Mater.* **2000**, *12*, 3301.

(7) (a) Kisler, J. M.; Dähler, A.; Stevens, G. W.; O'Connor, A. J. *Microporous Mesoporous Mater.* **2001**, *44–45*, 769. (b) Diaz, J. F.; Balkus Jr., K. J. *J. Mol. Catal. B: Enzymol.* **1996**, *2*, 115. (c) Deere, J.; Magner, E.; Wall, J. G.; Hodnett, B. K. *Chem. Commun.* **2001**, 465. (d) Deere, J.; Magner, E.; Wall, J. G.; Hodnett, B. K. *J. Phys. Chem. B* **2002**, *106*, 7340.

nm).<sup>5</sup> Due to their small pore size, MCM-41 structures are restricted to immobilization of enzymes with relatively small sizes.<sup>6</sup> In addition, relatively low enzyme loadings (typically <10 wt %) and slow enzyme immobilization rates are observed, despite these materials possessing surface areas as high as ca. 1000 m<sup>2</sup> g<sup>-1</sup>.<sup>6</sup> More recently, improved enzyme loadings have been reported for SBA-15 materials (pore sizes ca. 5–15 nm),<sup>8a</sup> and for mesocellular siliceous foam with pore sizes of 15–40 nm.<sup>8b</sup> The second issue pertaining to enzyme immobilization in MS is enzyme desorption; that is, substantial amounts (up to 70%) of the immobilized enzyme can desorb when the sample is dispersed/immersed in solution again. Such leaching can be attributed to the relatively weak physical adsorption between the enzyme and the silicious surface.<sup>6c</sup>

Recently, we reported a simple and versatile method to prepare high content enzyme-loaded particles by using MS spheres with sufficiently large pore sizes and volumes, bimodal MS (BMS) spheres with 10–40 nm pores and a pore volume of ca. 1.3 mL g<sup>-1</sup>.<sup>10</sup> We showed that the combination of using porous particles for enzyme immobilization and their subsequent coating with nanoscale multilayer shells to effect enzyme encapsulation overcomes the problem of enzyme desorption often encountered with the direct immobilization of enzymes on MSs. Additionally, improved enzyme stability and operational properties (i.e., recycling) were observed.<sup>10</sup>

In the current paper, we report in detail our studies on enzyme immobilization and encapsulation in BMS spheres, and the biocatalytic properties of the enzyme-loaded particles. The enzymes were immobilized on the MS spheres, and a multilayer shell was then assembled on the sphere surface by the layer-by-layer (LbL) electrostatic assembly of oppositely charged species (i.e., PE and silica nanoparticles (Si<sub>NP</sub>)) to encapsulate the enzyme (Figure 1). The enzyme immobilization capacity of the BMS particles was investigated for a range of enzymes with different sizes and isoelectric points (pI). Nonporous silica (NS) spheres and MS spheres with a series of pore sizes were also used as enzyme immobilization hosts for comparison. Two systems were used to form dense coatings on the enzyme-loaded BMS spheres: (i) a PE multilayer shell through the alternate deposition of poly(diallyldimethylammonium chloride (PDPA)) and poly(sodium 4-styrenesulfonate (PSS)); and (ii) a composite shell through the alternate deposition of PDPA and Si<sub>NP</sub>.

## Experimental Section

**Materials.** Poly(allylamine hydrochloride) (PAH,  $M_w$  15 000), poly(sodium 4-styrenesulfonate (PSS,  $M_w$  70 000), and poly(diallyldimethylammonium chloride (PDPA,  $M_w$  300 000–400 000) were obtained from Sigma-Aldrich. All PE solutions were of

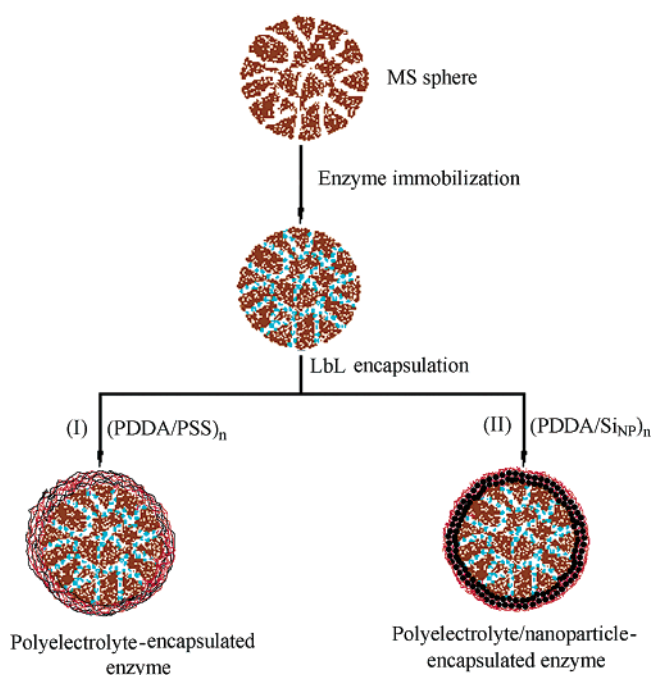


**Figure 1.** Schematic representation of enzyme encapsulation using MS spheres as supports. The enzyme is first immobilized and subsequently encapsulated by a (I) PE or (II) PE/nanoparticle multilayer shell.

concentration 3 mg mL<sup>-1</sup> and contained 0.5 M NaCl. Catalase (Sigma C-100, 42 300 units mg<sup>-1</sup> protein), protease (Sigma P6911, 5.2 units mg<sup>-1</sup> solid), peroxidase (POD, Sigma P8250), fluorescein isothiocyanate-labeled peroxidase (FITC-POD, Sigma P2649, extent of labeling 1–2 mol FITC per mol peroxidase), cytochrome C (Sigma C-2037), and lysozyme (Fluka BioChemika 62971) were dissolved in 50 mM phosphate buffer (PB) at a protein concentration of ca. 0.5 mg mL<sup>-1</sup>. Cetyltrimethylammonium bromide (CTABr), *n*-dodecylamine, *n*-hexadecylamine, poly(ethylene glycol)-*b*-poly(propylene glycol)-*b*-poly(ethylene glycol) (P<sub>123</sub>,  $M_w$  5800), sodium metasilicate (Na<sub>2</sub>SiO<sub>3</sub>), tetraethyl orthosilicate (TEOS, 98%), ammonia solution (25 wt % in water), and 2-propanol were used as received from Aldrich. The colloidal silica (Ludox AM-30, 30 wt % suspension in water) provided by DuPont was used as the Si<sub>NP</sub> source after dispersing in 0.1 M NaCl solution with a concentration of ca. 0.5 wt %. The water used in all experiments was prepared in a Millipore Milli-Q purification system and had a resistivity higher than 18.2 MΩ cm.

**Instrumentation.** Adsorption–desorption measurements were conducted on a Micromeritics ASAP 2000 apparatus at 77 K using nitrogen as the adsorption gas. The surface areas were calculated by the Brunauer–Emmett–Teller (BET) method, and the pore diameter distributions were derived from the adsorption branch by the Barrett–Joyner–Halenda (BJH) method. The particle morphologies were examined by scanning electron microscopy (SEM, Philips XL30, operated at 20 kV) and transmission electron microscopy (TEM, Philips CM120 BioTWIN, operated at 120 kV). The BMS particles were ultramicrotomed to a thickness of 90 nm for TEM measurement after embedding them in a LR white resin. ζ-Potentials were measured on a Zetasizer 2000 (Malvern) instrument. Confocal laser scanning microscopy (CLSM) images were taken with an Olympus confocal system equipped with a 60× oil immersion objective. A UV–vis (Agilent 8453) spectrophotometer was used to monitor the enzyme loading and for the enzyme activity assays.

**Preparation of BMS Spheres.** BMS particles were prepared according to the method outlined in the literature.<sup>11</sup> Briefly, 1.38 × 10<sup>-2</sup> mol of CTABr and 2.1 × 10<sup>-2</sup> mol of Na<sub>2</sub>SiO<sub>3</sub> were

- (8) (a) Fan, J.; Lei, J.; Wang, L.; Yu, C.; Tu, B.; Zhao, D. *Chem. Commun.* **2003**, 2140. (b) Lei, C.; Shin, Y.; Liu, J.; Ackerman, E. J. *J. Am. Chem. Soc.* **2002**, *124*, 11242. (c) Takahashi, H.; Li, B.; Sasaki, T.; Miyazaki, C.; Kajino, T.; Inagaki, S. *Microporous Mesoporous Mater.* **2001**, *44–45*, 755.
- (9) Han, Y.; Watson, J.; Stucky, G. D.; Butler, A. J. *Mol. Catal. B: Enzymol.* **2002**, *17*, 1.
- (10) Wang Y.; Caruso, F. *Chem. Commun.* **2004**, 1528.

dissolved to form a clear solution in 90 mL of Milli-Q water in a polyethylene bottle at 30 °C. Next, 6.4 mL of ethyl acetate was added, and the mixture was stirred for 30 s and allowed to stand at ambient temperature (20 °C) for 5 h. After this period of aging, the bottle was kept at 90 °C for 48 h in an oil bath. To obtain particles with a relatively narrow size distribution, larger particles ( $>4\ \mu\text{m}$ ) in the as-synthesized product were removed through repeated sedimentation steps.<sup>12</sup> The product (ca. 2–4  $\mu\text{m}$  BMS spheres) was collected by centrifugation (500g) and was washed with ethanol three times and then twice with Milli-Q water. The BMS particles contain domains with stable silica walls between the micelles as well as domains in which these walls are unstable or even missing, which form larger mesopores after the removal of surfactant micelles.<sup>11</sup>

**Preparation of NS and MS Spheres.** NS spheres (ca. 500 nm) were prepared by using a seeded-growth method.<sup>13</sup> First, 6 mL of TEOS was added to a solution containing 7 mL of ammonia solution (25 wt %), 1.8 mL of Milli-Q water, and 50 mL of ethanol under rapid stirring at ambient temperature. After 3 h, an additional 4 mL of TEOS was added, and the solution was stirred for a further 3 h. The MS spheres with mesopores in the range 2–3 nm were prepared using either *n*-dodecylamine or *n*-hexadecylamine as a template in a homogeneous phase of the water/alcohol cosolvent system.<sup>14,15</sup> MS spheres prepared using *n*-dodecylamine and *n*-hexadecylamine as templates are denoted as MS-12 and MS-16, respectively. For synthesis of the MS-12 spheres, 63 g of ethanol and 0.58 g of *n*-dodecylamine were added to 80 mL of Milli-Q water with rapid stirring and sonication for 5 min to form a clear solution. Following this, 1 mL of ammonia/2-propanol solution (25 wt % ammonia solution dissolved in 2-propanol with a concentration of 2.0 M) was added, and, after 10 min, 2.32 g of TEOS was added with vigorous stirring for a further 10 min. For preparation of the MS-16 spheres, *n*-dodecylamine (2.08 g) was dissolved in a mixture of 180 mL of Milli-Q water, 200 mL of 2-propanol, and 3.5 mL of ammonium hydroxide solution (25 wt %) to form a homogeneous solution. Afterward, 12 mL of TEOS was added with stirring, and the mixture was left standing overnight at ambient temperature (20 °C). The product was then collected by centrifugation (500g) and washing twice with Milli-Q water.

**Preparation of SBA-15.** SBA-15 was prepared by the method reported in the literature.<sup>16</sup> First, 2 g of P123 was dissolved in 15 mL of Milli-Q water at 30 °C, followed by the addition of 30 g of 2 M HCl solution and the dropwise addition of 4.4 g of TEOS. The mixture was stirred at 30 °C for 24 h, after which it was transferred into a Teflon bottle sealed in an autoclave. The sample was then heated to 100 °C for 48 h in an oven.

**Enzyme Immobilization.** Approximately 10 mg of the siliceous particles was dispersed in 10–20 mL of enzyme stock solution with a concentration of 0.5 mg mL<sup>-1</sup> in 50 mM PB at pH 7.0 and mixed at room temperature for a given time. The amount of enzyme

immobilized onto the particles was monitored by UV–vis spectrophotometry, that is, by measuring the enzyme absorbance before and after immobilization (after separating the supernatant via centrifugation). The bands used to monitor the immobilization of catalase, cytochrome C, POD, lysozyme, and protease were 405, 530, 403, 280, and 280 nm, respectively.

**Enzyme Encapsulation.** To demonstrate the encapsulation process and the enzyme properties after encapsulation, we employed catalase. Catalase is abundant in nature, decomposing hydrogen peroxide to water and molecular oxygen.<sup>17</sup> The catalase-loaded particles were washed with chilled (5 °C) PB solution twice before LbL coating. Adsorption of PDDA and PSS or SiNP was performed at 5 °C for 5 min with shaking. Excess PE or SiNP was separated by centrifugation (500g) and washing with a chilled 0.1 M NaCl solution three times. The SiNP dispersion, ca. 21 nm in diameter (measured by TEM and dynamic light scattering (DLS)), was used at a concentration of 0.5 wt % in 0.1 M NaCl solution. The encapsulated particles were finally dispersed in PB solution at a concentration of ca. 10 mg mL<sup>-1</sup>.

**Enzyme Activity Assay.** The enzyme activity was determined spectrophotometrically by using H<sub>2</sub>O<sub>2</sub> as a substrate.<sup>18</sup> Briefly, the encapsulated enzyme (or free enzyme) was added to 11 mM H<sub>2</sub>O<sub>2</sub> in 50 mM PB solution with rapid stirring. The decrease in absorbance at 240 nm (with an extinction coefficient of 0.041 mmol<sup>-1</sup> cm<sup>-1</sup>) with time was recorded immediately after the enzyme was mixed into the above solution at 20 °C.<sup>18</sup> One unit of catalase will decompose 1  $\mu\text{mol}$  of H<sub>2</sub>O<sub>2</sub> per minute at pH 7.0 and 20 °C.

**Encapsulated Enzyme Stability.** Enzyme leakage after immobilization and/or encapsulation was examined by dispersing 5.0 mg of sample in 5.0 mL of 50 mM PB (pH 7.0) and shaking at 37 °C for 6 h. The amount of catalase released was calculated by measuring the supernatant activity after centrifuging. To determine the stability of catalase after encapsulation, 10 mg of the biocatalyst (catalase encapsulated in the BMS spheres) was dispersed in 10 mL of 11 mM H<sub>2</sub>O<sub>2</sub> in PB (50 mM, pH 7.0). After H<sub>2</sub>O<sub>2</sub> consumption, centrifugation, and removal of the supernatant, 10 mL of fresh substrate solution was added for the next reaction cycle.

**Proteolysis Experiments.** First, 20 mg of protease was dissolved in 1.0 mL of PB solution at pH 7.0 and used as a stock solution. Next, 0.2 mL of the free catalase, the BMS sphere-immobilized catalase, or the BMS sphere-encapsulated catalase (the initial catalase activity was ca. 10 000 units mL<sup>-1</sup> for all samples) was separately incubated in a water bath at 37 °C with either 40  $\mu\text{L}$  of the protease stock solution or 40  $\mu\text{L}$  of PB (control experiment). Proteolysis of the catalase was determined by measuring the activity decrease of catalase through decomposition of H<sub>2</sub>O<sub>2</sub>.

## Results and Discussion

**Silica Sphere Properties.** BMS spheres of size between 2 and 4  $\mu\text{m}$  were used for enzyme encapsulation (Figure 2a). The inner structure of the BMS spheres was examined by TEM on ultramicrotomed samples (ca. 90 nm thick slices) of the spheres (Figure 2b,c). Figure 2b shows that the inside of each BMS particle is relatively homogeneous. The apparent larger size distribution (0.8–3.5  $\mu\text{m}$ ) is caused by slicing of the BMS particles through random sections. At higher magnification, the disordered pore structure with pore sizes of 10–40 nm becomes apparent (Figure 2c). Nitrogen

- (11) Schulz-Ekloff, G.; Rathouský, J.; Zukal, A. *Int. J. Inorg. Mater.* **1999**, *1*, 97.
- (12) The as-synthesized BMS particles were dispersed in Milli-Q water with a concentration of ca. 0.5 wt %. Next, 80 mL of the BMS sphere suspension was pipetted into a test tube of diameter 2 cm and length 20 cm. The tube was placed vertically in a rack and left for ca. 10 min to allow the larger particles to sediment. The suspension above the sedimented particles was then recovered and placed in a new tube. These separation steps were repeated five times.
- (13) Konno, M.; Inomata, H.; Matsunaga, T.; Saito, S. *J. Chem. Eng. Jpn.* **1994**, *27*, 134.
- (14) Nooney, R. I.; Thirunavukkarasu, D.; Chen, Y.; Josephs, R.; Ostafin, A. E. *Chem. Mater.* **2002**, *14*, 4721.
- (15) Grun, M.; Buchel, C.; Kumar, D.; Schumacher, K.; Bidingmaier, B.; Unger, K. K. *Stud. Surf. Sci. Catal.* **2000**, *128*, 155.
- (16) Zhao, D.; Feng, J.; Huo, Q.; Melosh, N.; Fredrickson, G. H.; Chmelka, B. F.; Stucky, G. D. *Science* **1998**, *279*, 548.

- (17) Lu, J. R.; Swann, M. J.; Peel, L. L.; Freeman, N. J. *Langmuir* **2004**, *20*, 1827.
- (18) Mannheim, B. *Biochemica Information*, 1st ed.; 1987; p 15.



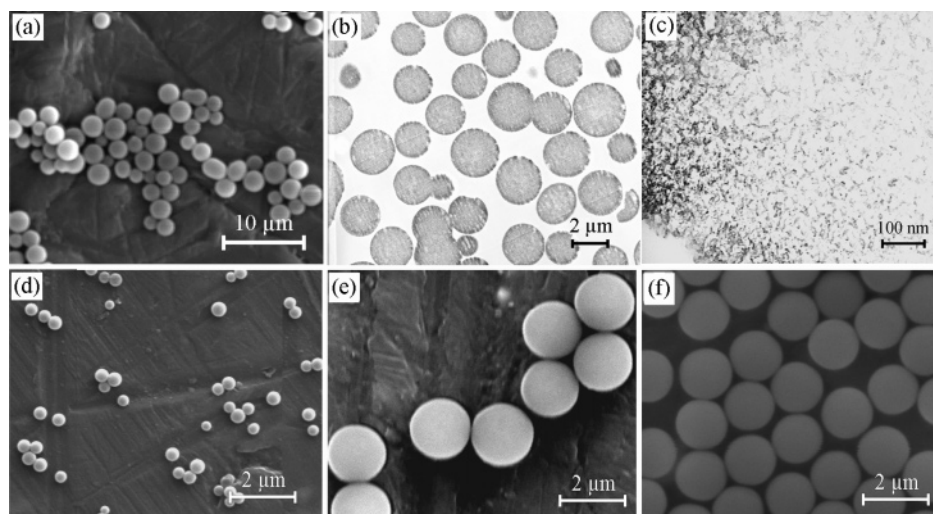


**Figure 2.** Electron microscopy images of the silica spheres employed: (a) SEM images of the BMS spheres and (b, c) TEM of ultramicrotomed samples of the BMS spheres; SEM images of the (d) NS spheres, (e) MS-12 spheres, and (f) MS-16 spheres.

**Table 1. Properties of the Particles Used for Enzyme Immobilization and Encapsulation**

samples	average particle size / $\mu\text{m}$	surface area / $\text{m}^2 \text{g}^{-1}$	average pore size /nm	pore volume / $\text{cm}^3 \text{g}^{-1}$
BMS	$2.5 \pm 0.5$	630	2–3, 10–40 <sup>a</sup>	1.7
NS	$0.5 \pm 0.1$	6.7 <sup>b</sup>	<sup>c</sup>	<sup>c</sup>
MS-12	$1.8 \pm 0.1$	1080	2.0	0.60
MS-16	$1.2 \pm 0.1$	800	2.3	0.65
SBA-15	<sup>d</sup>	845	6.8	1.2

<sup>a</sup> Bimodal pore distribution. <sup>b</sup> Calculated on the basis of a silica density of  $1.8 \text{ g cm}^{-3}$ . <sup>c</sup> Nonporous. <sup>d</sup> Powder.

adsorption results show that the BMS material has a surface area of  $630 \text{ m}^2 \text{g}^{-1}$  and a pore volume of  $1.72 \text{ cm}^3 \text{g}^{-1}$  (Table 1). From the pore distribution curve (Figure 3b), it can be seen that the material has a bimodal pore structure, that is, smaller pores in the 2–3 nm range, and the larger pores ranging from 10 to 40 nm with a volume of  $1.28 \text{ cm}^3 \text{g}^{-1}$ . The larger mesopores facilitate encapsulation of biomacromolecules such as enzymes. For comparison, NS spheres (Figure 2d), MS spheres with only small mesopores (ca. 2–3 nm) (Figure 2e,f), and SBA-15 with a pore size of ca. 7 nm were also used as supports for enzyme immobilization. The properties of the particles used are summarized in Table 1. The MS-12 and MS-16 particles were prepared in a homogeneous phase; hence the particle size (Figure 2e,f) and pore distribution (Figure 3b) are more homogeneous than those measured for the BMS particles. The SBA-15 possesses a noodle-like morphology (not shown).<sup>16</sup>

**Enzyme Immobilization.** To investigate the potential of BMS spheres for biomacromolecule uptake, several model enzymes with different molecular weights and pI were employed. The particles were exposed to the enzyme solution for a set time, and the enzyme content retained by the particles was determined by recording the difference in enzyme solution absorbance before and after immobilization experiments. The enzyme loadings are summarized in Table 2. High loadings (20–40 wt %, 200–400  $\text{mg g}^{-1}$ ) were observed for BMS particles for the enzymes with low molecular weight and high pI (e.g., cytochrome C, lysozyme, and protease). Electrostatic forces have typically been used to entrap proteins in MS materials because silica has a pI of

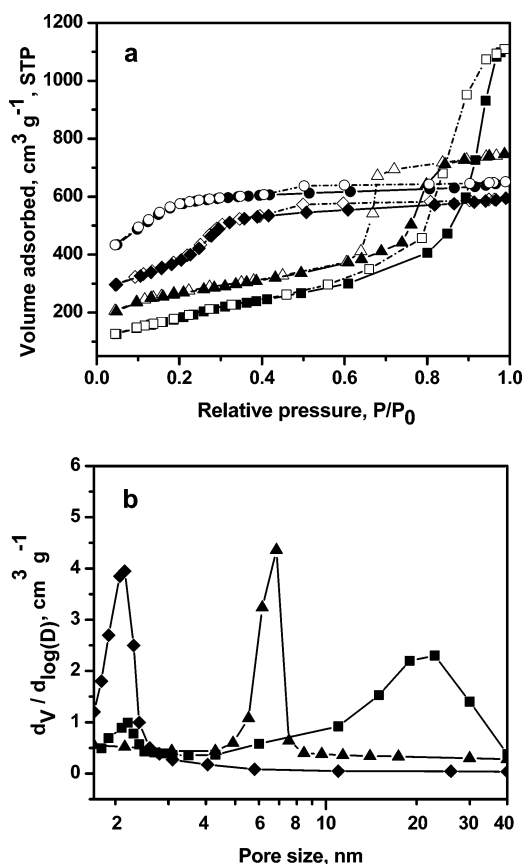


**Figure 3.** (a) Nitrogen sorption isotherms and (b) pore distributions of the BMS spheres (squares), MS-12 spheres (circles), MS-16 spheres (diamonds), and SBA-15 (triangles). No pore distribution is shown for the MS-12 spheres. The open symbols and dashed lines in the nitrogen sorption isotherms correspond to the desorption branches.

ca. 3.<sup>6–9</sup> At several pH units away from the pI of the enzyme, electrostatics provide a driving force for enzyme immobilization. For the MS-12 and MS-16 spheres, the enzyme loading for cytochrome C, lysozyme, and protease ranges from ca. 10 to 120  $\text{mg g}^{-1}$ , while for the NS spheres it ranges from ca. 2 to 8  $\text{mg g}^{-1}$ . When the enzyme pI is close to the solution conditions used for immobilization (pH 7), discernment of the factor(s) driving protein adsorption is often difficult because there commonly exists a number of interactions (e.g.,

Table 2. Enzyme Properties and Immobilized Amounts on Siliceous Particles with Different Porosity

enzyme	$M_w$ /kDa	size /nm	pI	enzyme immobilized amount /mg g <sup>-1</sup> <sup>a</sup>				
				BMS	NS	MS-12	MS-16	SBA-15
cytochrome C	12	3.0	10.3	231	4.6	28	37	160
lysozyme	14.6	3.0–4.5	11	397	7.5	99	120	450
protease	20			203	4.8	13	22	126
POD	44	4.8	8	48	0.9	1.8	2.6	7.9
catalase	250	10.4	5.4	75	5.2	7.5	7.5	15

<sup>a</sup> The loadings correspond to the amount of enzyme immobilized per gram of particles at saturation adsorption, calculated from UV–vis measurements. The error in these values is less than 5%. Conditions used for enzyme immobilization were 50 mM PB solution (pH 7) and an enzyme concentration of 0.5 mg mL<sup>-1</sup>.

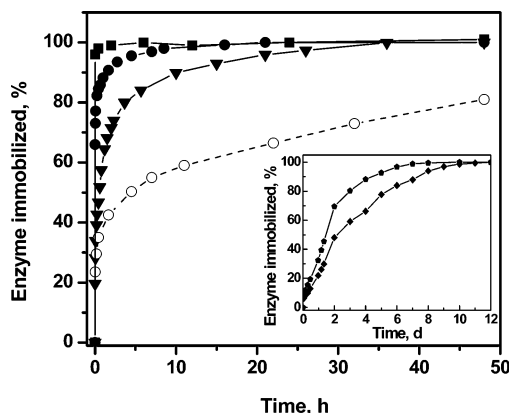


**Figure 4.** Comparison of the normalized lysozyme immobilization rate on NS (squares), BMS (filled circles), SBA-15 (triangles), MS-16 (pentagons), and MS-12 (diamonds) particles as a function of adsorption time. The inset corresponds to adsorption isotherms of lysozyme on MS-16 (pentagons) and MS-12 (diamonds) particles (x-axis: d = days). The solution conditions were 0.5 mg mL<sup>-1</sup> lysozyme, pH 7.0, 50 mM PB, and 20 °C. The immobilization rate of catalase in BMS spheres (dashed line, open circles) under the same conditions is also shown.

electrostatics, hydrogen bonding, and van der Waals forces) operating simultaneously. For immobilization of the larger enzyme with a lower pI (i.e., POD) onto BMS spheres, the enzyme loading decreases (ca. 50 mg g<sup>-1</sup>). Catalase has a larger molecular size (ca. 10 nm) than POD (ca. 5 nm) and a net negative charge at pH 7.0 (pI 5.4).<sup>19</sup> Approximately 75 mg g<sup>-1</sup> of catalase is immobilized onto BMS particles. This value is ca. 15, 10, and 5 times larger than the immobilized amount on and in the NS spheres, MS spheres, and SBA-15, respectively. The higher immobilized amounts in the BMS particles are attributed to the larger pore sizes in BMS than those of the other materials (see Table 1).

The pore size of the siliceous spheres has a significant influence on the rate of enzyme immobilization (Figure 4). For BMS particles, ca. 85% of saturation loading is achieved within 15 min for lysozyme, with adsorption saturating in ~10 h. For the SBA-15, MS-16, and MS-12 particles, lysozyme adsorption reaches saturation at ca. 40 h, 7 days, and 10 days, respectively. These data are similar to those reported for lysozyme immobilization in MCM-41 materials.<sup>7a</sup> In contrast to porous particles, lysozyme reaches adsorption saturation quickly (<5 min) on the NS spheres, but with a low loading (ca. 8 mg g<sup>-1</sup>). This is consistent with lysozyme adsorption being restricted to immobilization on the particle surface for the NS spheres. Furthermore, the enzyme size also plays a significant role in the immobilization rate; for example, catalase requires ca. 5 days to reach adsorption

equilibrium in the BMS spheres. Although SBA-15 shows a high capacity to load the smaller enzyme lysozyme (ca. 450 mg g<sup>-1</sup>), its loading ability for catalase (ca. 15 mg g<sup>-1</sup>) is considerably lower than that of the BMS particles (ca. 75 mg g<sup>-1</sup>).

The immobilization and distribution of enzyme in the BMS particles were examined by CLSM. Figure 5 shows the CLSM images of the BMS and MS-12 spheres after incubation in FITC-POD for 60 min, followed by washing with copious amounts of Milli-Q water. The bright spheres seen are due to the homogeneous distribution of FITC-POD in the BMS particles (Figure 5a), reflecting the effective immobilization of POD molecules within the pores of the particles. For the MS-12 particles, distinct fluorescent rings are observed, indicating localization of most of the POD on the sphere surface (Figure 5b). The fluorescence intensity originating from the MS-12 sphere surface is significantly lower than that observed from the BMS particles, which is consistent with lower POD loadings observed for the MS-12 spheres (see Table 2). To investigate the pore interconnectivity of the MS-12 particles, the smaller fluorescent dye Rhodamine 6G ( $M_w$  479) was adsorbed in the MS spheres. Bright spheres with a homogeneous fluorescence distribution were observed after Rhodamine 6G loading (Figure 5b inset), confirming that the pores in MS-12 are well connected. This clearly shows that the low enzyme loading in the MS-12 spheres can be ascribed to the relatively small mesopores in comparison to the larger mesopore distribution (10–40 nm) of the BMS particles.

The high enzyme immobilization capacity of the BMS spheres was verified by the color variation of the particles following exposure to enzyme solutions (Figure 6). Cytochrome C and catalase solutions show a red and brown-green color, respectively. The white BMS and SBA-15 particles turn deep red after exposure to cytochrome C solution (Figure 6c), while the MS-16 particles assume a pale red color over 4 days (Figure 6b). Although the average pore size of MS-16 particles (ca. 2 nm) is smaller than the diameter of cytochrome C (ca. 3 nm), a cytochrome C loading of 3.7 wt % in MS particles was still obtained after incubating for 4 days. This might be caused by the protein penetrating into the smaller pores through configuration/morphology variations. A small number of mesopores that are larger than the cytochrome C diameter are also possibly included in the MS-16 particles. For the NS spheres, no obvious color change was found, even after 10 days of incubation in a cytochrome C solution (Figure 6a). For the larger enzyme catalase, which has a diameter of ca. 10 nm, only the BMS particles showed

(19) Product information is available from the Sigma-Aldrich website.

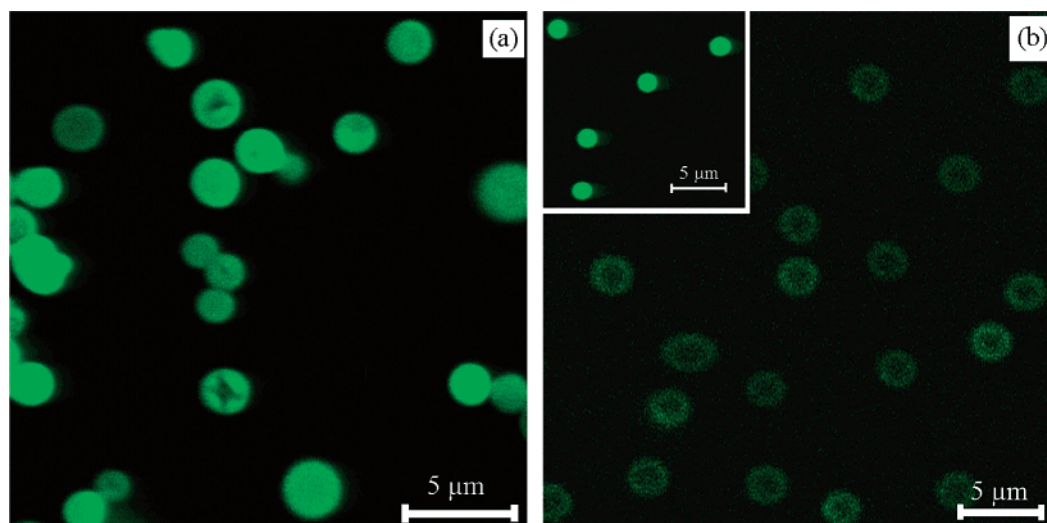


**Figure 5.** CLSM images of FITC-POD-loaded (a) BMS spheres and (b) MS-12 spheres. The inset in (b) corresponds to Rhodamine 6G-loaded MS-12 spheres.

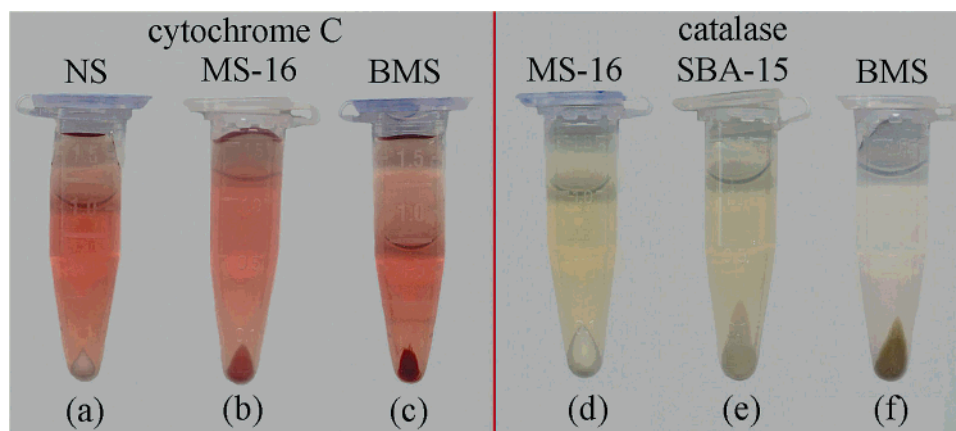


**Figure 6.** Photographs illustrating the color changes of the particles following the immobilization of cytochrome *C* (a–c) or catalase (d–f) onto NS (a), MS-16 (b, d), BMS (c, f), and SBA-15 (e) particles.

a stark color change (deep brown-green color) after 5 days of incubation (Figure 6f). After exposure to catalase solutions, SBA-15 particles showed a slight change in color because they have a pore size of ca. 7 nm (Figure 6e), while no distinguishable color change was observed for the MS-16 spheres (Figure 6d), which have much smaller pores. These results show that BMS particles have a higher capacity than the NS spheres, MS spheres, and SBA-15 for cytochrome *C* and catalase immobilization.

**Enzyme Encapsulation.** Substantial amounts of enzyme adsorbed in the pores can be desorbed when the sample is again dispersed in solution because of the relatively weak physical attraction between the enzyme and MSs.<sup>6c</sup> To prevent enzyme desorption from the BMS supports, and to provide a protective barrier for the loaded enzyme (for example, as desired in environments where enzyme-degrading substrates such as proteases may be present), a multilayer shell was assembled on the BMS sphere surface following enzyme loading. As depicted in Figure 1, PDDA/PSS or PDDA/SiNP shells were deposited. To demonstrate the encapsulation process, we employed catalase as a model system. Encapsulated catalase has useful applications in various areas such as the food industry (for the removal of hydrogen peroxide from food products after cold pasteuriza-

tion),<sup>20</sup> the textile industry (for the degradation of hydrogen peroxide after textile bleaching),<sup>21</sup> and the analytical field (as a sensor for hydrogen peroxide and glucose).<sup>22</sup>

The successive growth of the multilayer shells on the BMS particles was monitored by following the  $\zeta$ -potential changes of the particles after each deposition step. Figure 7 shows the  $\zeta$ -potential as a function of PE or SiNP layer number. The original BMS spheres have a  $\zeta$ -potential of ca.  $-40$  mV and ca.  $-30$  mV after catalase immobilization. As expected, the presence of a single layer of adsorbed positively charged PDDA on the BMS particles causes a reversal in  $\zeta$ -potential to positive values, and subsequent deposition of the PSS or SiNP layer reverts the  $\zeta$ -potential to negative values. These alternating trends in  $\zeta$ -potential are similar to those obtained previously for the same multilayer coatings<sup>23</sup> and qualitatively demonstrate the successful deposition of each PE and SiNP layer.

(20) Arica, M. Y.; Oktem, H. A.; Oktem, Z.; Tuncel, S. A. *Polym. Int.* **1999**, *48*, 879.

(21) (a) Weck, M. *Text. Prax. Int.* **1991**, *2*, 144. (b) Stober, R.; Petry, R. *Melliand Textilber.* **1995**, *11*, 1010.

(22) Choi, M. M. F.; Yiu, T. P. *Enzyme Microb. Technol.* **2004**, *34*, 41.

(23) (a) Caruso, F.; Caruso, R. A.; Möhwald, H. *Science* **1998**, *282*, 1111. (b) Caruso, F.; Möhwald, H. *J. Am. Chem. Soc.* **1999**, *121*, 6039.



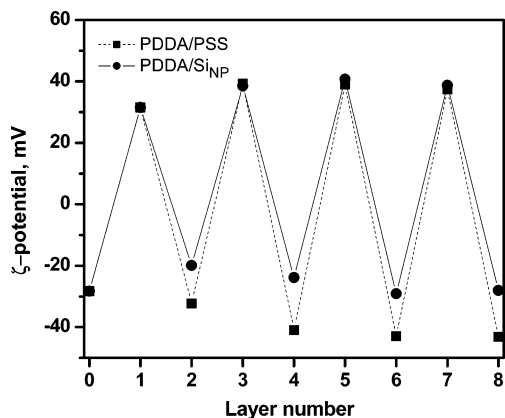


**Figure 7.** Variation in the  $\zeta$ -potential for the deposition of PDPA/PSS or PDPA/SiNP multilayer shells on catalase-loaded BMS spheres. The  $\zeta$ -potential measurements were performed in Milli-Q water at pH 5.8. Layer number 0 corresponds to the catalase-loaded BMS spheres. Layer numbers 1, 3, 5, and 7 correspond to PDPA deposition, and layer numbers 2, 4, 6, and 8 correspond to PSS (squares) or SiNP (circles) deposition.

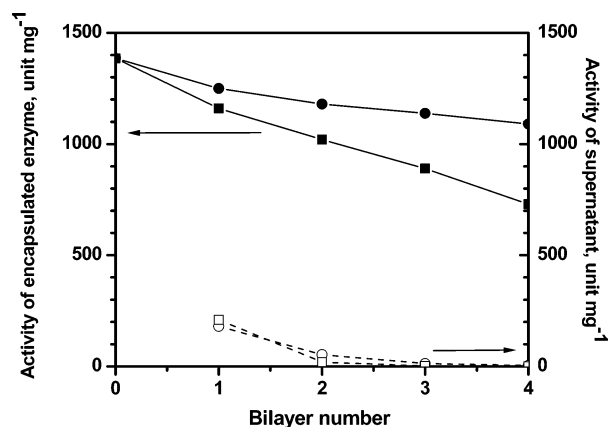


**Figure 8.** Specific activity of catalase immobilized on BMS spheres and encapsulated by PDPA/PSS (filled squares) or PDPA/SiNP (filled circles) multilayers. The activity of the corresponding amount of enzyme released during assembly of the multilayer coating is also shown (open squares and open circles). The enzyme activities are calculated on the basis of the BMS sphere weight. The lines are drawn to guide the eye.

The amount of catalase desorbed from the BMS particles during the encapsulation process was measured by monitoring the enzyme activity in the supernatant solution. The activity was determined by measuring the kinetics of  $\text{H}_2\text{O}_2$  decomposition in a stirred system, according to standard procedures.<sup>18</sup> The reaction rate is extremely fast, and under optimum conditions one mole of catalase is able to decompose  $5 \times 10^8$  mol of  $\text{H}_2\text{O}_2$  per min,<sup>19</sup> which makes the measurement very sensitive to small amounts of catalase released during multilayer shell formation. Approximately 12% of the immobilized catalase was released from the BMS particles as a result of deposition of a single layer of PDPA. This may be caused by the competitive adsorption between PDPA and catalase for the negatively charged silica surface, and the formation of PDPA and catalase complexes in solution. Enzyme leakage during shell formation dramatically decreases for subsequent PE or SiNP deposition steps. No detectable catalase activity in the supernatant was observed after the deposition of three bilayers (Figure 8). The encapsulation of enzyme was further examined via enzyme-leakage experiments, which involved incubating the particles in PB solution at 37 °C for 6 h. No enzyme was detected in

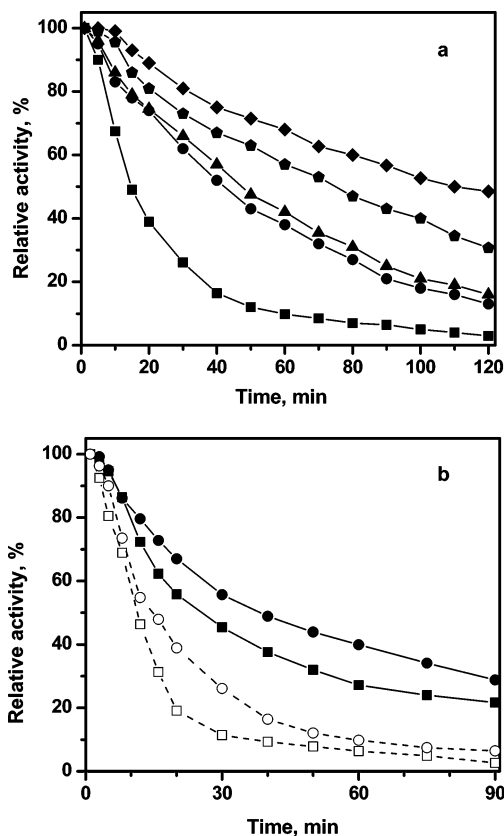


**Figure 9.** Relative activity as a function of reaction time: (a) free catalase (squares), catalase loaded in BMS particles (circles), catalase loaded in BMS particles coated with two (triangles), four (pentagons), and six (diamonds) PDPA/PSS bilayers; (b) free catalase at pH 5.1 (open squares) and pH 7.0 (closed squares), catalase loaded in BMS particles coated with three PDPA/SiNP bilayers at pH 5.1 (open circles) and pH 7.0 (closed circles).

the supernatant after incubating the catalase-loaded BMS particles coated with (PDPA/PSS)<sub>3</sub> or (PDPA/SiNP)<sub>3</sub>, whereas ca. 25% of the loaded catalase desorbed from the uncoated BMS particles.

The activity of catalase-loaded BMS spheres was dependent on the type of layers used for encapsulation and on the number of layers deposited. For the same number of layers, the enzyme activity was lower when PDPA/PSS layers were used for encapsulation as compared to PDPA/SiNP layers (Figure 8). However, the stability was higher for catalase encapsulated by PDPA/PSS layers (Figure 9a), rather than PDPA/SiNP layers (Figure 9b). Catalase immobilized in BMS particles and encapsulated by PDPA/SiNP has a stability similar to that of catalase solely immobilized in BMS particles and shows no dependency on layer number. In contrast, there is a direct relationship between enzyme stability and layer number for PDPA/PSS-encapsulated catalase-loaded BMS particles (BMS spheres with catalase and coated with 2, 4, and 6 bilayers of PDPA/PSS yielded an activity of 15%, 29%, and 47%, respectively, after 120 min (Figure 9a)). The enhanced lifetime may be caused by a reduced reaction rate as a result of the PE multilayers.<sup>24a</sup> This finding is in agreement with our previous work on catalase immobilization onto three-dimensional intercon-

(24) (a) Jin, W.; Shi, X.; Caruso, F. *J. Am. Chem. Soc.* **2001**, *123*, 8121. (b) Caruso, F.; Trau, D.; Möhwald, H.; Renneberg, R. *Langmuir* **2000**, *16*, 1485.

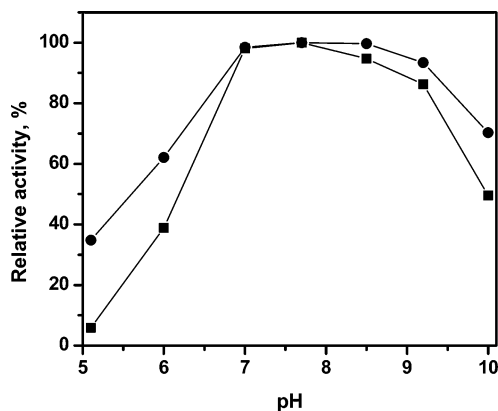


**Figure 10.** Relative activity of catalase as a function of pH: catalase in solution (squares); catalase loaded in BMS spheres coated with three PDDA/SiNP bilayers (circles). The activity at pH 7.0 was normalized to 100%.

nected macroporous zeolitic membranes, in which the catalase lifetime was also significantly enhanced after PE multilayer coating.<sup>25</sup> For the PDDA/SiNP coatings, sufficiently large pores still remain between the closely packed silica nanoparticles,<sup>23</sup> thus enabling faster diffusion of the substrate and product (oxygen) than through the PE coatings.

The catalase encapsulated in the BMS spheres has a higher activity over a wider pH range than “free” enzyme in solution (Figure 10). At pH 5.1, the free catalase has an activity of ca. 5% relative to the optimum enzyme activity at pH 7, while the encapsulated (or immobilized) enzyme has a relative activity of ca. 35%. The enzyme lifetime is also enhanced after encapsulation (Figure 9b). The activity decreased to ca. 5% for free catalase after 1 h at pH 7, while the encapsulated enzyme retained ca. 40% of its original activity.

Catalase encapsulated in the NS, MS-12, and BMS spheres coated with three bilayers of PDDA/SiNP has an activity of 12, 15, and 1138 units  $\text{mg}^{-1}$ , respectively. Although the amount of catalase adsorbed on BMS particles is about 10–15 times larger than that adsorbed on the NS and MS spheres (see Table 2), the activity of the enzyme encapsulated in the BMS spheres is over 75-fold larger than that observed for the NS and MS particles. This is caused by a larger extent of desorption of the immobilized enzyme (assessed by measuring the enzyme activity in the supernatant) from the NS and MS-12 materials during the PDDA and SiNP coating, because catalase is mainly adsorbed on the surface of these particles.

The activity of the encapsulated catalase and the stability imparted by the shell coating with respect to proteolysis were also examined (Figure 11). Free catalase was inactivated immediately by protease, losing its entire activity within ca. 60 min (a). For catalase immobilized in BMS spheres, inactivation is slightly slower (20% activity after 60 min) (b). Notably, the enzyme stability is significantly higher for the (PDDA/SiNP)<sub>3</sub>-coated BMS sphere-catalase particles (50% of the original activity was retained after 90 min) (c), and even higher for the (PDDA/PSS)<sub>4</sub>-coated BMS sphere-catalase particles (~98% activity after 120 min) (d). Because protease has a high affinity to BMS particles and its

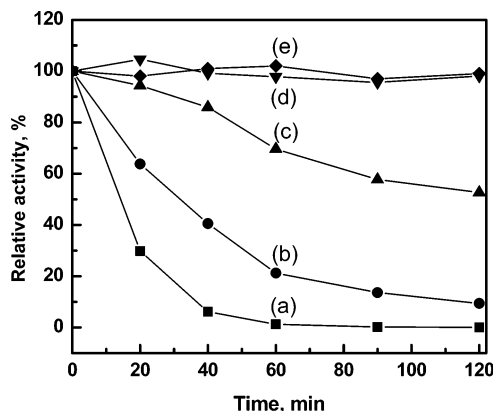


**Figure 11.** Stability (in the presence of protease) of (a) free catalase, (b) catalase loaded in BMS particles, (c) catalase loaded in BMS particles coated with three PDDA/SiNP bilayers, (d) catalase loaded in BMS particles coated with four PDDA/PSS bilayers, and (e) catalase loaded in BMS particles coated with three PDDA/SiNP bilayers and four PAH/PSS bilayers.

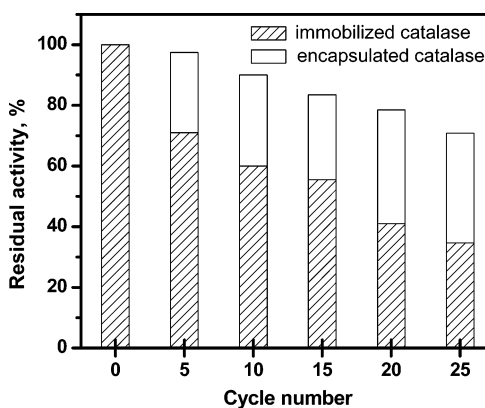


**Figure 12.** Activity of catalase immobilized and encapsulated in BMS particles coated with three PDDA/SiNP bilayers as a function of successive batch reactions.

molecular weight is relatively small (see Table 2), some protease may still penetrate the porous PDDA/SiNP coating. The pure PE multilayer shells, on the other hand, can form a dense shell with micropores, through which only small molecules (molecular weight below ~4000) can penetrate (under the assembly conditions employed).<sup>26,27</sup> Enhanced protection for the encapsulated enzyme was obtained by depositing four additional PAH/PSS bilayers on the (PDDA/SiNP)<sub>3</sub>-encapsulated catalase in BMS spheres (e).

An advantage of the enzyme-loaded BMS spheres is their reusability. The activity of catalase encapsulated in the BMS particles with PDDA/SiNP layers decreased by only ca. 4% after recycling five times (Figure 12). Significantly more activity (ca. 30%) was lost if the enzyme was only immobilized in the BMS particles. After 25 successive batch reactions, the immobilized and encapsulated catalase showed activities of 35% and 70%, respectively. The lower activity observed for the immobilized catalase is caused by enzyme leakage during the multiple soaking, separation, and washing steps employed during the recycling process.

## Conclusions

We have described an effective method to encapsulate enzymes by using MS particles with pore sizes between 10



and 40 nm for enzyme immobilization, and subsequent stepwise coating with nanoscale shells. The BMS particles display significantly improved enzyme immobilization capacity and a faster immobilization rate than MS spheres with only 2–3 nm pores. Enzyme loadings in the range 20–40 wt % were obtained for small enzymes (diameter ca. 3 nm) with a high pI ( $>10$ ) and ca. 8 wt % for larger enzymes such as catalase. Encapsulation resulted in enhanced enzyme properties, as evidenced by experiments with catalase. The lifetime of catalase was improved when encased by LbL assembled PE or composite (PDDA/Si<sub>NP</sub>) shells on the catalase-loaded BMS spheres. The encapsulated catalase can also be recycled 25 times with an associated loss of activity of 30%, as compared to the 65% loss in activity for catalase immobilized in the BMS spheres. Additionally, ca. 98% of the activity of the encapsulated catalase was retained when subjected to proteolysis treatment. The enzyme-loaded

particles prepared are likely to find application in catalysis, as they can act as efficient and stable biocatalysts. They also may serve as useful building blocks to construct biofunctional thin films with high enzyme loadings. Furthermore, the approach presented can be extended to encapsulate other macromolecules (e.g., polyelectrolytes) and nanoparticles in MS materials. Such studies are the focus of our current investigations.

**Acknowledgment.** This work was supported by the Australian Research Council (Discovery Project and Federation Fellowship Schemes) and the Victorian State Government, Department of Innovation, Industry and Regional Development, Science, Technology and Innovation initiative. We thank B. Radt for the CLSM measurements, and A. Yu for helpful discussions.

CM0483137